

Asian dust events of April 1998

R. B. Husar,¹ D. M. Tratt,² B. A. Schichtel,¹ S. R. Falke,¹ F. Li,¹ D. Jaffe,³ S. Gassó,³ T. Gill,⁴ N. S. Laulainen,⁵ F. Lu,⁶ M. C. Reheis,⁷ Y. Chun,⁸ D. Westphal,⁹ B. N. Holben,¹⁰ C. Gueymard,¹¹ I. McKendry,¹² N. Kuring,¹⁰ G. C. Feldman,¹⁰ C. McClain,¹⁰ R. J. Frouin,¹³ J. Merrill,¹⁴ D. DuBois,¹⁵ F. Vignola,¹⁶ T. Murayama,¹⁷ S. Nickovic,¹⁸ W. E. Wilson,¹⁹ K. Sassen,²⁰ N. Sugimoto,²¹ and W. C. Malm²²

Abstract. On April 15 and 19, 1998, two intense dust storms were generated over the Gobi desert by springtime low-pressure systems descending from the northwest. The windblown dust was detected and its evolution followed by its yellow color on SeaWiFS satellite images, routine surface-based monitoring, and through serendipitous observations. The April 15 dust cloud was recirculating, and it was removed by a precipitating weather system over east Asia. The April 19 dust cloud crossed the Pacific Ocean in 5 days, subsided to the surface along the mountain ranges between British Columbia and California, and impacted severely the optical and the concentration environments of the region. In east Asia the dust clouds increased the albedo over the cloudless ocean and land by up to 10–20%, but it reduced the near-UV cloud reflectance, causing a yellow coloration of all surfaces. The yellow colored backscattering by the dust eludes a plausible explanation using simple Mie theory with constant refractive index. Over the West Coast the dust layer has increased the spectrally uniform optical depth to about 0.4, reduced the direct solar radiation by 30–40%, doubled the diffuse radiation, and caused a whitish discoloration of the blue sky. On April 29 the average excess surface-level dust aerosol concentration over the valleys of the West Coast was about 20–50 $\mu\text{g}/\text{m}^3$ with local peaks $>100 \mu\text{g}/\text{m}^3$. The dust mass mean diameter was 2–3 μm , and the dust chemical fingerprints were evident throughout the West Coast and extended to Minnesota. The April 1998 dust event has impacted the surface aerosol concentration 2–4 times more than any other dust event since 1988. The dust events were observed and interpreted by an ad hoc international web-based virtual community. It would be useful to set up a community-supported web-based infrastructure to monitor the global aerosol pattern for such extreme aerosol events, to alert and to inform the interested communities, and to facilitate collaborative analysis for improved air quality and disaster management.

1. Introduction

Extreme biogeochemical events such as volcanic eruptions, forest fires, and dust storms provide unique opportunities to examine the inner workings of the atmospheric system. Such

events tend to produce large quantities of dust, smoke, or haze, which are then dispersed over regional or global scales. The easily observable atmospheric particles can visualize and quantify the nature of transport, transformation, and removal processes along their path. An early benefit of aerosols as visualizers of global transport was the discovery of the global circulation of the atmosphere after the Krakatoa volcanic eruption in 1883 [Symons, 1888]. The volcanic stratospheric aerosol and red sunsets observed all around the globe led to the recognition of the organized global circulation pattern.

¹Center for Air Pollution Impact and Trend Analysis, Washington University, St. Louis, Missouri.

²Jet Propulsion Laboratory, California Institute of Technology, Pasadena, California.

³Atmospheric Sciences, University of Washington, Seattle, Washington.

⁴Department of Geosciences, Texas Tech University, Lubbock, Texas.

⁵Pacific Northwest National Laboratory, Richland, Washington.

⁶National Satellite Meteorological Center, China Meteorological Administration, Beijing, China.

⁷U.S. Geological Survey, Washington, D. C.

⁸Meteorological Research Institute, Seoul, Republic of Korea.

⁹Naval Research Laboratory, Monterey, California.

¹⁰NASA Goddard Space Flight Center, Greenbelt, Maryland.

¹¹University of Central Florida, Orlando, Florida.

¹²Department of Geography, University of British Columbia, Vancouver, British Columbia, Canada.

¹³Scripps Institution of Oceanography, University of San Diego, La Jolla, California.

¹⁴Center for Atmospheric Chemistry Studies, University of Rhode Island, Kingston, Rhode Island.

¹⁵Air Quality Bureau, New Mexico Environment Department, Santa Fe, New Mexico.

¹⁶Solar Monitoring Laboratory, University of Oregon, Eugene, Oregon.

¹⁷Department of Physics, Tokyo University of Mercantile Marine, Tokyo, Japan.

¹⁸Euro-Mediterranean Centre on Insular Coastal Dynamics (ICoD), University of Malta, Valletta, Malta.

¹⁹National Center for Environmental Assessment, U.S. Environmental Protection Agency, Research Triangle Park, North Carolina.

²⁰Department of Meteorology, University of Utah, Salt Lake City, Utah.

²¹National Institute for Environmental Studies, Tsububa, Ibaraki, Japan.

²²NPS Air Resources Division, CIRA, Colorado State University, Fort Collins, Colorado.

Copyright 2001 by the American Geophysical Union.

Paper number 2000JD900788.
0148-0227/01/2000JD900788\$09.00

Clearly, the atmospheric particles from extreme events are not mere neutral tracers and visualizers but are also major carriers in the biogeochemical cycle of sulfur, nitrogen, carbon and trace metals, as well as crustal elements. Last but not least, dust, smoke, and haze particles produced by these processes influence climate and weather, oceanic and terrestrial fertility, and impact public health.

Dust storms in deserts of east Asia tend to cause major aerosol events well beyond the Asian continent. The eruption of volcanoes, major forest fires, and large dust storms are often associated with catastrophic consequences to humans and their environment, but the prediction of their specific occurrence in space and time is virtually impossible. The unpredictability of these events also presents a unique challenge to atmospheric research, since sustained readiness for intensive field campaigns is almost impossible to maintain. Hence the study of such events generally has to rely on the integration of routine monitoring data and serendipitous observations.

The transport of desert dust from Asia to the North Pacific atmosphere is well documented [e.g., Shaw, 1980; Duce et al., 1980; Parrington et al., 1983; Uematsu et al., 1983; Merrill et al., 1989; Bodhaine, 1995; Husar et al., 1997] and results in a maximum in aerosol loading each spring. Over the Pacific the concentration of species from anthropogenic sources in Asia was also found to be enhanced during spring [Prospero and Savoie, 1989; Jaffe et al., 1997; Talbot et al., 1997] and has been documented to reach North America [Jaffe et al., 1999].

Compelling geological evidence of global scale transport of Asian dust emerged from the chemical analysis of samples in the Greenland ice core [Biscaye et al., 1997] and Hawaiian soil studies [Rex et al., 1969; Dymond et al., 1974; Kennedy et al., 1998; Chadwick et al., 1999]. The chemical and radiological fingerprints of deposited dust at both locations were most consistent with the composition of the Asian dust sources.

This paper reports the formation, transport, and other characteristics of two dust storms in April 1998. The focus is on the dust storm that occurred April 19, 1998, over the Gobi desert (Mongolia and north central China), which crossed the Pacific causing aerosol concentrations near the health standard ($150 \mu\text{g}/\text{m}^3$) over much of the West Coast of North America.

Several observers in Asia and North America monitored the unusual dust cloud independently. In Japan, for example, an integrated lidar monitoring network was operated in anticipation of the springtime dust (kosa) season [Murayama et al., this issue]. At the Center for Air Pollution Impact and Trend Analysis (CAPITA), Washington University, the dust cloud was detected as a distinct yellow cloud on the daily SeaWiFS color satellite images using the web-based NASA Goddard SeaWiFS Global Browser facility. The dust was also independently observed over the western Pacific on GOES 9 geostationary satellite images [Bachmeier, 1998].

When it was evident that the Asian dust cloud was reaching North America, an interactive website was set up on April 26 at CAPITA, Washington University (<http://capita.wustl.edu/Asia-FarEast/>) to register various observations, to exchange opinions, and to support general communication and data sharing (cooperation) among the interested observers. By April 29, through word of mouth, over 40 scientists and air quality managers from North America and Asia had registered with the ad hoc work group and began sharing their data and qualitative observations with the spontaneously formed open virtual community. Most participants maintained their shared data and preliminary reports on their own web pages, but the

CAPITA web site supported a user-maintained central catalog of web resources along with an open discussion forum. The first phase of the virtual work group activity was completed with a preliminary summary of the dust event that was web-published on May 11, 1998. In December 1999 the virtual workgroup was reactivated to produce this research paper. This *Journal of Geophysical Research* issue contains several other papers prepared independently on various aspects of these dust events. Given the broad and multifaceted nature of this report, the observations are presented chronologically following the evolution of the two dust clouds.

2. Observations of April 1998 Dust Events

The dust events were observed through routine satellite sensors, lidar instruments, Sun photometers, airborne samplers, and a large array of surface-based aerosol monitors on both sides of the Pacific.

2.1. Remote Sensing of Dust Events

Satellite remote sensing data delivered daily through the web were crucial in detecting the dust clouds, following their evolution as well as characterizing the spatial, temporal, and optical characteristics of the moving dust clouds. Daily spectral images of the dust cloud from the SeaWiFS sensor [McClain et al., 1998; Barnes et al., 1999] provided detailed spatial and spectral patterns of the dust at about local noon each day. On the SeaWiFS images, the dust cloud was recognized by its bright yellow color, partial transparency, and smooth spatial texture. The raw (Level 1A) SeaWiFS data were obtained from the SeaWiFS Program [McClain et al., 1998] and processed at Washington University. The resulting spectral reflectance values (fraction of radiation reflected) represented the combined reflectance from the land, clouds, and the aerosol. The scattering by air molecules was removed from the total reflectance using the Vermote and Tanre [1992] procedure, which also included nominal corrections for ozone and water vapor absorption.

The on-line, hourly, GMS-5 geostationary satellite data with visible and IR channels were used for near-continuous monitoring of the dust plume dynamics throughout the day. Visible images from geostationary satellites (GOES 8, GOES 10, and GMS-5) were effective for dust detection during the twilight hours when the Sun was in front of the sensor. At dawn or dusk the reflectance from the ground surface is minimal, while the reflectance from the aerosol is still high. This, along with forward scattering from the Sun, tends to produce a strong amplification of the aerosol-scattering signal.

During the postanalysis of the dust episode, operational retrievals of absorbing aerosol index from the TOMS (Total Ozone Mapping Spectrometer) satellite [Herman et al., 1997] provided useful information on the daily spatial distribution of the dust cloud. The TOMS aerosol-absorbing signal is a semi-quantitative index of the columnar absorption by aerosols at $0.340 \mu\text{m}$. The signal is derived from the absorption of the upwelling Rayleigh scattering from the lower strata of the atmosphere. The April 1998 dust clouds over Asia were also detected using the AVHRR (advanced very high resolution radiometer) sensor by the "split window" method, taking the difference between the 11 and $12 \mu\text{m}$ channels [Murayama et al., this issue]. Routine quantitative techniques for the retrieval of aerosol properties over land from satellite data are not yet available, but it is an area of active research [King et al., 1999].

For this reason the satellite data are used here for characterizing the change in surface reflectance (albedo) due to the dust rather than for aerosol optical thickness retrieval.

The vertical optical thickness was detected by Sun photometers as part of the AERONET (Aerosol Robotic Network) network in Asia and in North America [Holben *et al.*, 1998], by the Solar Radiation Monitoring Laboratory, University of Oregon [Gueymard *et al.*, 2000], and by a number of other Sun photometer networks.

The vertical dust profiles were monitored by lidar instruments on both sides of the Pacific. The passage of the April 15 dust cloud over Japan was monitored by a coordinated network of lidar instruments [Murayama *et al.*, this issue] sited throughout Japan, augmented by Sun photometers and surface concentration measurements. The dust cloud was detected over North America as part of the routine long-term monitoring program of the aerosol vertical structure conducted by the CO₂ backscatter lidar facility at the Jet Propulsion Laboratory [Tratt and Menzies, 1994]. Timely alerts provided by the “virtual community” through the web site allowed normal operations at this facility to be optimally focused on observation of the extreme dust event. Lidar observations of the Asian dust cloud were also reported from the University of Utah as part of their cirrus cloud-monitoring program [Sassen, 1997].

2.2. In Situ Measurements

The detailed physical, chemical, and optical characteristics of the April 1998 dust aerosol were recorded by surface-based in situ measurements and aircraft samplings. Daily visibility observations around the Gobi desert provided an indication of reduced visibility due to the dust as well as the cause of the obstruction to vision, i.e., dust [National Climate Data Center (NCDC), 1998].

Continuous aerosol size distribution data using an optical counter were reported from Korea [Chun *et al.*, 2000]. More than 200 PM10 samplers were located throughout the West Coast states of North America. These samplers collected particulate mass less than 10 μm in size, some operating hourly, others collecting 24 hour samples [EPA, 1994]. Full network sampling was conducted every sixth day with limited coverage (25–30 samplers) during the intervening periods. The composition of the fine particle (PM2.5) dust aerosol for chemical fingerprinting was captured in great detail by over 50 stations of the IMPROVE (Interagency Monitoring of Protected Visual Environments) network that sampled twice a week, Wednesdays and Saturdays [Malm *et al.*, 1994].

3. Formation of Dust Clouds Over Gobi Desert

Dust clouds are formed when the friction from high surface wind speeds (>5 m/s) lifts loose dust particles into the atmospheric boundary layer or above [Gillette, 1978]. Windblown dust originating from the arid deserts of Mongolia and China is a well-known springtime meteorological phenomenon throughout east Asia. In fact, “yellow sand” meteorological conditions are sufficiently common to have acquired local names: huangsha in China, whangsa in Korea, and kosa in Japan. The Asian dust storms have been studied for decades to understand their sources, mechanisms of transport, and aerosol characteristics, including the effects on radiation [Mizohata and Mamuro, 1978; Zhou *et al.*, 1981; Wang *et al.*, 1982; Iwasaka *et al.*, 1983; Zaizen *et al.*, 1995; Zheng *et al.*, 1998; Zhang and Lu, 1999]. However, quantitative understanding of

individual dust events, for example, the dust emission locations and rates as well as the details of long-range transport and removal, are still incomplete.

To gain a broader perspective on the formation of the Gobi dust clouds in April 1998, the daily time series of three measured dust indices were examined over the regions shown in Figure 1a. Figure 1b depicts the time series of (1) the TOMS satellite data averaged over the Gobi desert as a regional index of total suspended dust, (2) the average surface extinction coefficient based on eight synoptic visibility monitoring stations (a measure of the ground-level dust concentration), and (3) the aerosol optical thickness measured at Dalamzagdud, Mongolia, showing quantitatively the total dust extinction in the vertical column.

Figure 1c shows the daily TOMS aerosol index averaged over the much larger east Asia region. Figure 1d shows the dust emission rate, while Figure 1d presents the concentration of suspended dust particles (diameter <10 μm) aggregated over east Asia using the Naval Research Laboratory (NRL) global aerosol model by Westphal [2000]. The NRL model is based on the Christensen [1997] hemispheric Eulerian model. It uses the NRL forecast meteorological fields [Hogan and Rosmond, 1991] and customized emissions for sulfur, windblown dust, and biomass smoke.

The two peaks in the daily time series of the aerosol concentration indices over the Gobi desert region (Figures 1b and d) convey that two major dust storms occurred on April 15 and 19, respectively. Furthermore, the TOMS data (Figure 1c) and the model simulations of suspended dust averaged over east Asia (Figure 1e) indicate that the April 19, 1998, storm was the more intense event causing higher regional average dust concentrations. The synoptic scale pressure and wind fields for April 15 and 19 are shown in Figures 1f and 1g. In what follows, the two dust events are examined in more detail, including a comparison of the two storms.

4. April 15 Dust Cloud

4.1. Formation

Analysis of meteorological data and modeling results [Nickovic *et al.*, this issue; Westphal, 2000] indicate that the formation of April 15 was associated with cold weather systems with high surface wind speeds. Figure 1f shows that on April 15 a low-pressure system (<995 mbar) was passing over eastern Mongolia. A strong high-pressure system (>1025 mbar) was located over western Mongolia. The extreme pressure gradient resulted in the high (20 m/s) winds over the Gobi desert.

The most detailed spatial distribution of the dust was obtained from the 1 km resolution SeaWiFS satellite images. Plates 1a–1d depict the dust pattern on April 15 and 16. The spectral reflectance images from SeaWiFS provide a rich visual context, including surface reflectance and the position of white cloud systems relative to the yellow dust. For comparison the contour of the TOMS absorbing aerosol index (green line, aerosol index = 2) was superimposed on the spectral SeaWiFS images.

On the satellite images depicting the April 15 cloud (Plate 1b) the sources can be identified as streaks of dust plumes originating from specific patches of land, presumably from sand dunes or loess not covered by vegetation. Dust plumes are evident on both sides of the Mongolia-China border in the Gobi desert. After about 500 km of transport the plumes merged, and the streaky plume structure disappeared.

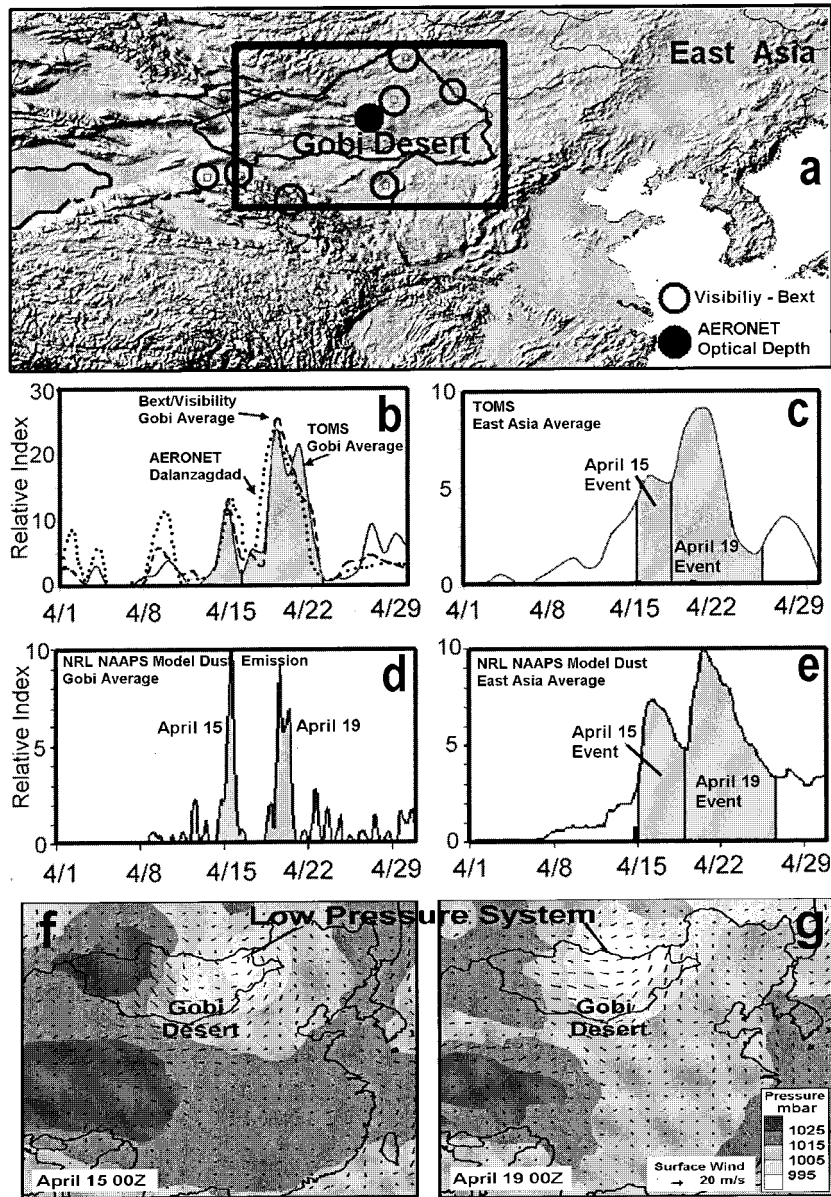


Figure 1. Daily variation of aerosol during April 1998. (a) Map of the geographic areas for the Gobi desert region and east Asia. (b) Daily aerosol variation over the rectangular Gobi region for visibility-derived horizontal extinction coefficient averaged over nine stations, AERONET Sun photometer aerosol optical thickness for Dalanzagdad, and regional average TOMS signal. (c) Daily time series of the TOMS aerosol index averaged over east Asia. (d) Simulated lifted dust over the Gobi region [Westphal, 2000]. (e) Simulated suspended dust over east Asia [Westphal, 2000]. The data show an aerosol peak on April 15 and a much larger peak starting April 19, 1998. (f) Surface pressure and wind fields on April 15, 1998. (g) Surface pressure and wind fields on April 19, 1998.

4.2. Transport and Spatial Distribution

The April 15, 1998, dust cloud followed a southern route toward central and eastern China and subsequently turned toward Korea to the north. The location of the dust plume is visualized using the superimposed SeaWiFS and TOMS data in Plate 1. On April 16 the dust plume reached the populated eastern seaboard of China between Beijing and Shanghai (Plate 1c). Plate 1d also illustrates in more detail that even after about 1000 km of transport from the Gobi desert the dust plume has retained considerable spatial texture. In addition, at the leading edge, the dust cloud is delineated by a sharp front,

while the dust level in the tail section is decaying more gradually. The highest dust reflectance is found adjacent to the clouds, which suggests dust entrainment into the precipitation cloud system over Korea.

The superposition of the TOMS and SeaWiFS data in Plate 1 reveals that on April 15 the dust pattern from TOMS and SeaWiFS did not coincide geographically. This is an indication that the fresh dust layer was near the ground where the TOMS sensor is less sensitive to dust. This is consistent with the lidar data for the April 15 event collected over eastern China, Korea, and Japan [Murayama *et al.*, this issue], indicating a gen-

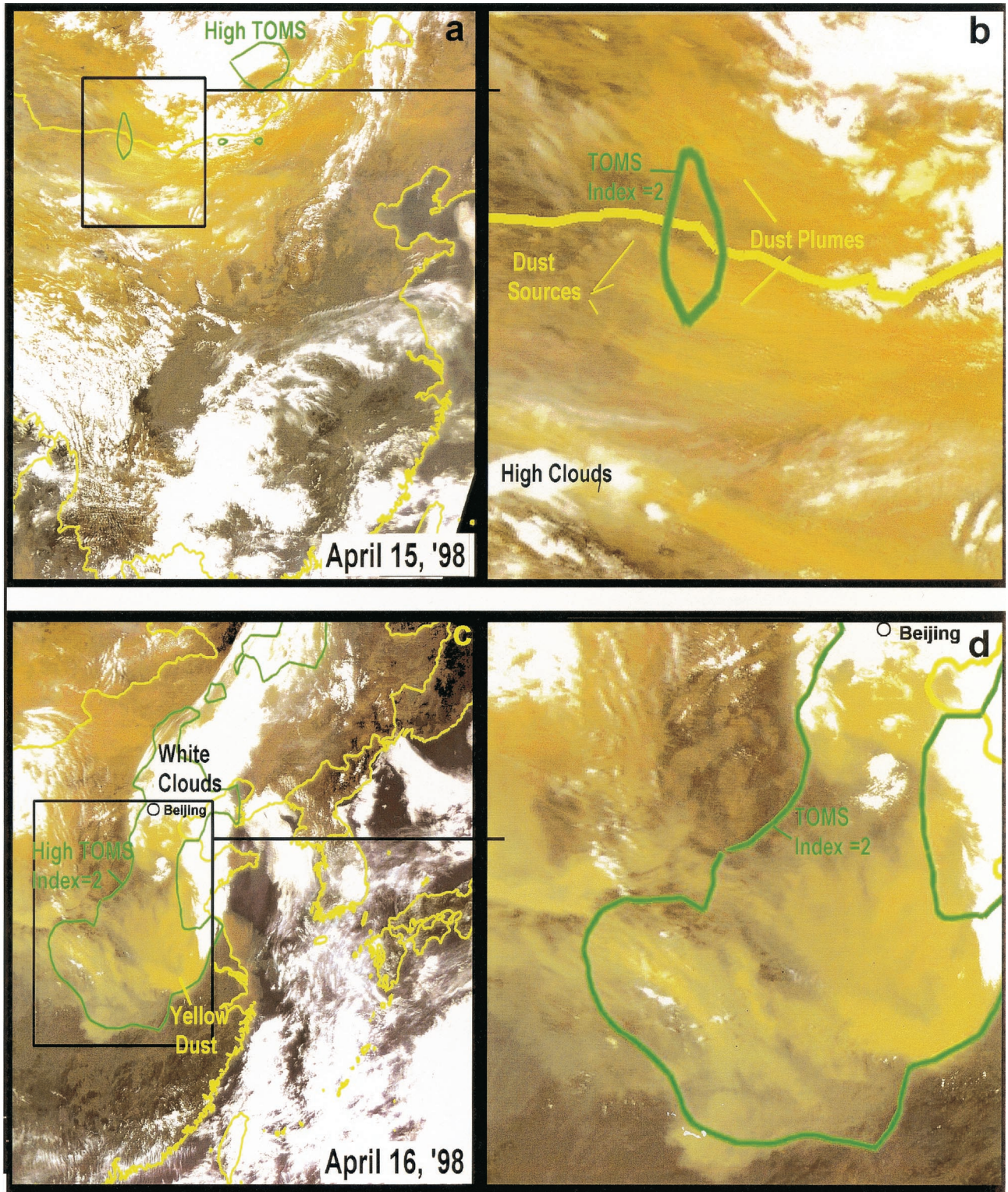


Plate 1. (a, b) SeaWiFS and TOMS satellite data for the April 15 and (c, d) April 16. The quantitative SeaWiFS reflectance (albedo) data are rendered as “true color” using the blue ($0.412 \mu\text{m}$), green ($0.550 \mu\text{m}$), and red ($0.670 \mu\text{m}$) channels. The scattering by air molecules was removed. The TOMS absorbing aerosol index (level 2.0) is superimposed as green contours. The yellow dust is distinguishable from the white clouds and dark land surfaces.

erally well-mixed dust layer from the surface to about 3 km. On April 16 (Plates 1c and 1d) the spatial patterns of the SeaWiFS and TOMS signals coincide, possibly due to deeper mixing of the dust layer. The TOMS data indicate that on April 19 (Plate

2a), remnants of the April 15 dust cloud were present over the Yellow Sea and Korea, but the SeaWiFS data show virtually no excess reflectance over the same location. A full explanation of the SeaWiFS-TOMS differences is not yet available.

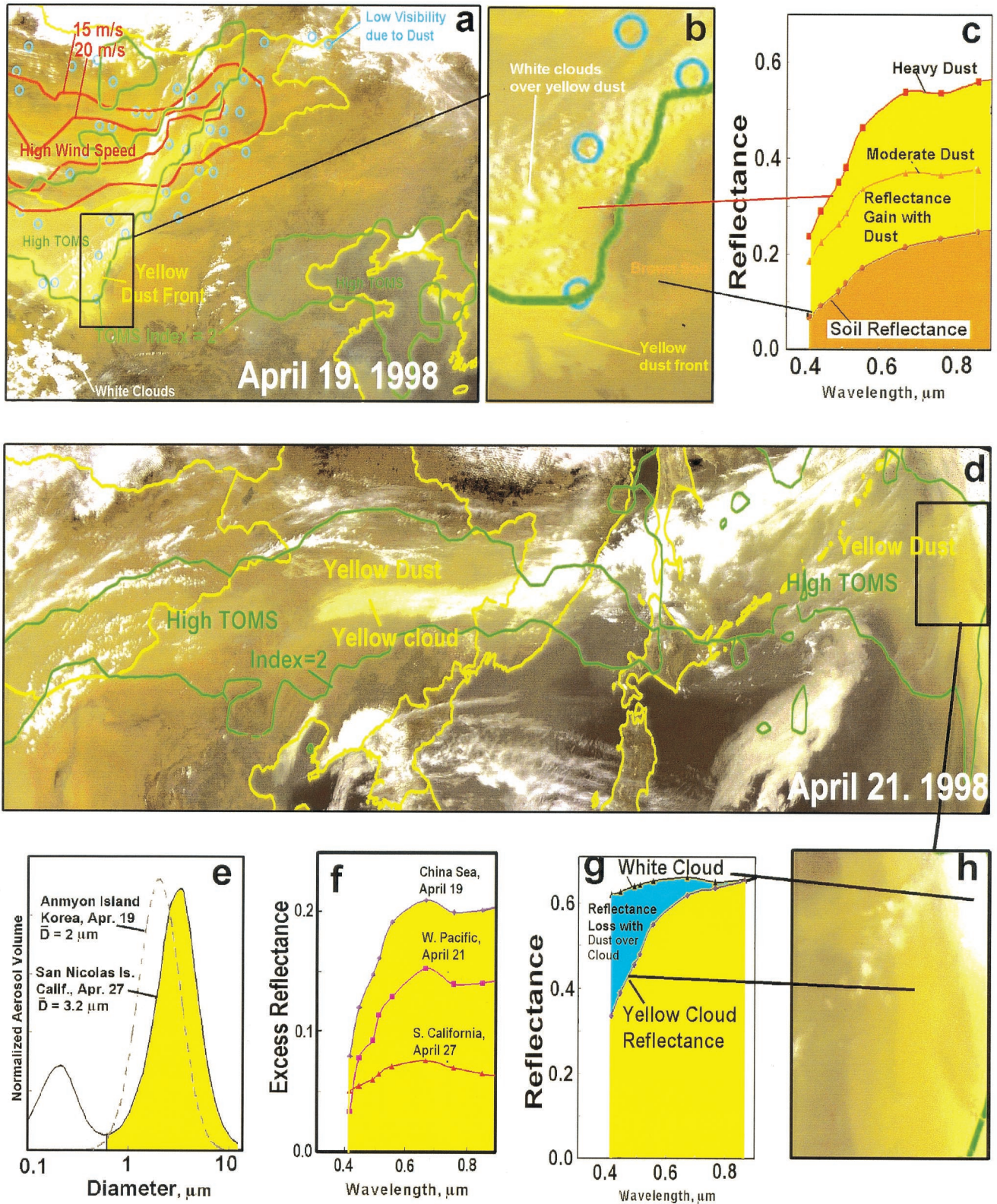


Plate 2. (a, b) SeaWiFS and TOMS satellite data for the April 19 and (d, h) April 21. (a) The April 19 image also contains the surface wind speed contours and surface visibility data. (b) Detail of the dust front. (c) Surface reflectance spectra over land with and without dust. (e) Dust volume distribution function at Anmyon Island in Korea and at San Nicolas Island in California. (f) Excess spectral reflectance of dust over ocean. (g) Loss of cloud reflectance due to yellow dust.

4.3. Dissipation

The dust cloud dissipates when the particles are removed from the atmosphere by dry and wet removal processes. Gravitational settling of large particles ($>10 \mu\text{m}$) occurs near the source within the first day of transport. Wet removal occurs sporadically throughout the 5–10 day lifetime of the remaining smaller-size dust particles. Dispersion by vertical, axial, and lateral mixing of air masses is responsible for the dilution of dust concentration. The available data do not establish how and where the Asian dust cloud is ultimately dissipated, i.e., removed from the atmosphere. However, various dust aerosol observations allow drawing of a limited number of inferences about the removal processes that affected the dust.

Throughout much of its residence over east Asia the April 15 dust cloud was embedded either in or near a precipitating low-pressure system, as illustrated in Plate 1. Consequently, the dust cloud appears to have been strongly depleted by wet removal processes throughout much of its residence over East Asia. On April 16, Beijing was under a thick cloud cover, but yellow dust was visible just to the south (Plate 1c). On April 16 and 17 the newspapers in Beijing, China, also reported yellow muddy rain (F. Li, personal communication, 1998). Yellow muddy rain with a relatively high pH value (6.22) was reported on April 17 in Korea [*Korean Meteorological Research Institute (KMRI)*, 2000]. However, detailed rain chemical composition data for the April 15 dust events are not available at this time.

The dust size distribution measured on Anmyon Island, Korea, on April 19 evidently characterized the aged dust emitted on April 15. The measured volume size distribution function (Plate 2e) shows a sharp peak between 1 and $5 \mu\text{m}$, with a volume-mean diameter of $2 \mu\text{m}$ and a logarithmic standard deviation of 1.6 [*Chun et al.*, 2000]. Continuous monitoring of particle concentration in different size ranges exhibited a strong correlation between the particles in the dust peak size range ($2\text{--}3 \mu\text{m}$) and virtually no correlation with particles below $0.8 \mu\text{m}$ and above $10 \mu\text{m}$. Hence the size ranges below $0.8 \mu\text{m}$ and above $10 \mu\text{m}$ have different origins than the coherent dust size range between 1 and $10 \mu\text{m}$ [*Chun et al.*, 2000]. The absence of transported large particles implies that the dust particles above $10 \mu\text{m}$ were preferentially removed by gravitational settling during the 2–3 day atmospheric transport time from Gobi to Korea. On the basis of the meteorological conditions and satellite images it is presumed that the April 15, 1998, dust cloud was removed from the atmosphere over east Asia without substantial transport across the Pacific.

5. April 19 Dust Cloud

5.1. Formation

Analysis of meteorological data and modeling results [*Nickovic et al.*, this issue; *Westphal*, 2000] indicate that on April 19 a major storm swept through Mongolia and north central China. The dust storm was driven by a low-pressure cold front that entered western Mongolia and swiftly moved eastward (Figure 1g). On April 19 the surface wind speeds increased to over 20 m/s as shown in the wind speed contours in Plate 2a. This was well above the generally assumed threshold wind speed (5–6 m/s) for dust suspension [*Gillette*, 1978]. On April 15 as well as on April 19 the region of high wind speeds coincided with the Gobi desert in southern Mongolia and the adjacent loess plateau in the Gansu province of China. However, in the April 19 image (Plate 2a) the individual dust plumes were not apparent.

Rather, a dense and sharp dust front is evident at the leading edge of the dust cloud (Plate 2b).

A superposition of the TOMS and SeaWiFS data in Plate 2a indicates that on April 19 the dust pattern from TOMS and SeaWiFS coincides geographically. This implies that the dust layer was higher than on April 15, since in this case the TOMS sensor detected it.

5.2. Transport and Pattern Over Asia

The transport of the April 19 dust cloud was due east over eastern Mongolia, toward the Pacific. Plate 2 shows the position of the dust cloud on April 19 and 21, respectively. By April 20 (not shown) the leading edge of the dust cloud reached the Pacific, and by April 21 (Plate 2d) the yellow dust cloud was stretching more than 1000 km into the Pacific Ocean.

The location of the dust cloud was also observed in surface visibility data reported by the global synoptic network. On April 19, the visibility was reduced throughout central and eastern Mongolia as indicated by the blue circles in Figure 3. Over 30 visibility stations reported dust as the cause for the obstruction to vision. The vertical optical thickness of the suspended dust measured in Dalanzagdad, Mongolia (B. N. Holben, personal communication, 1999) indicated that the turbidity increased from $\tau < 0.5$ on April 18 to $\tau > 2$ on April 19 as the dust cloud passed by. In addition, the measured spectral optical thickness was virtually constant between 0.4 and $1.02 \mu\text{m}$ ($\alpha \sim 0$) (B. N. Holben, 1999), which indicates a characteristic size in excess of $2 \mu\text{m}$.

In the SeaWiFS reflectance data (Plates 1 and 2) the dust is recognized by its distinctly yellow color. Plate 2c shows the spectral reflectance function over soil with and without the dust cloud. Evidently, the presence of the thick atmospheric dust increases the soil reflectance more in the red (from 0.25 to 0.55) than in the blue (from 0.05 to 0.3). Consequently, the dust appears brighter and more yellow than the underlying soil.

Dust layers were also frequently observed above low-lying white clouds, imparting a yellow hue to the clouds. It is presumed that the yellow coloration is due the scattering and absorption of the superimposed dust layer. Plates 2g and 2h show the spectral reflectance of clouds with and without the dust layer. The “white” cloud had a spectrally flat reflectance of about 0.65, while the “yellow” clouds show a similar reflectance at $0.67 \mu\text{m}$ but only 0.35 at $0.412 \mu\text{m}$. The resulting spectral reflectance curve for the yellow clouds is similar but somewhat higher than the reflectance of dust over soil.

The dust also appears yellow in color over the dark cloud-free ocean surface, as shown in Plate 2f. Near the dust source over the China Sea and western Pacific the excess dust reflectance (in excess of the reflectance of aerosol-free ocean) is in the range 0.1–0.2 above $0.5 \mu\text{m}$ wavelength, but it drops sharply below this wavelength. In fact, even a thick dust layer reflects only about 7% of the incoming solar radiation at $0.412 \mu\text{m}$.

These observations indicate that an elevated dust layer causes a yellow coloration of all surfaces, regardless whether it is dark land or ocean or bright soil and white clouds. Radiative calculations indicate that the spherical Mie scattering assumption with constant imaginary refractive index cannot explain the phenomenon, but the relative roles of particle spectral absorption in the near UV and of irregular particle shape are not clear. The sharp drop in near-UV dust reflectance eludes plausible explanation, but the yellow dust color served well for dust visualization.

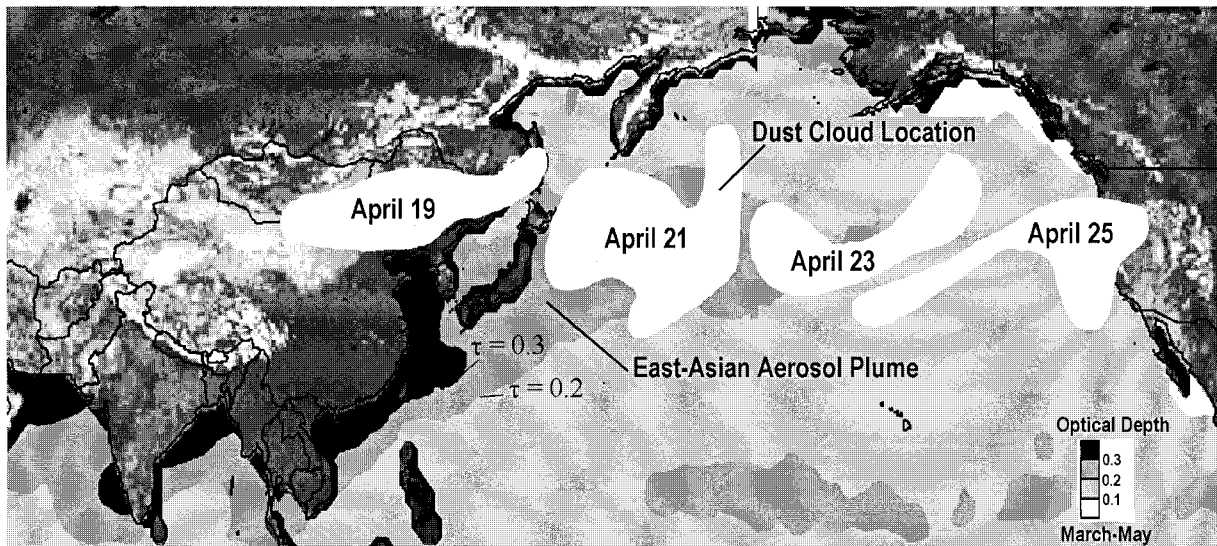


Figure 2. Approximate location of the April 19 dust cloud over the Pacific Ocean between April 21 and 25. The daily dust patterns were derived from the SeaWiFS images, GOES 9 and GOES 10 images, and TOMS absorbing aerosol index data. Over the Pacific Ocean the dust cloud followed the path of the springtime east Asian aerosol plume shown by the contours of optical thickness derived from AVHRR data.

5.3. Transport Across the Pacific

Once the dust cloud reached the Pacific Ocean, it was carried by the westerly winds that are typical for the northern midlatitudes (30° – 60° N) in the springtime. The dust transport path across the Pacific was visualized on the SeaWiFS images by the yellow dust itself. During the trans-Pacific transport, the approximate daily location of the dust cloud is shown in Figure 2. It is based on the visual examination of the daily SeaWiFS, TOMS, and GOES satellite images. It is remarkable that the dust cloud reached the West Coast of North America within 5–6 days after the emissions, corresponding to 12 m/s average transport speed.

It is evident that during the trans-Pacific passage the dust cloud was stretched longitudinally. Also, large segments of the dust cloud were peeled off and transported northward into the Arctic reducing the amount of dust reaching North America. Model simulations [Westphal, 2000; Nickovic *et al.*, this issue] also show such piecemeal disintegration of the dust cloud.

As a reference, Figure 2 also shows the contours of the springtime seasonal average (March–May) aerosol optical depth over the Pacific Ocean derived from the AVHRR sensor [Husar *et al.*, 1997]. Evidently, the April 1998 dust cloud trajectory roughly coincided with the seasonal average seasonal aerosol plume emanating from east Asia.

The height at which the dust traversed the Pacific is not well documented. The yellow discoloration of the clouds near the coast of China on April 21, Plate 2d, indicates that at least part of the dust layer was above the low-lying white clouds. Similar qualitative observations over the Pacific also indicate that some of the dust was above the cloud layers. The fast (>12 m/s) trans-Pacific transport also implies that the dust layer must have been well above the marine boundary layer. Unfortunately, the April 19 dust storm passed to the north of the east Asian lidar network, so lidar profiles are not available.

5.4. Asian Dust Over North America

The earliest record of the arrival of the April 19 Asian dust to North America was late on April 24 by the lidar at the

Facility for Atmospheric Remote Sensing in Salt Lake City, Utah. The dust layer detected at Salt Lake City occurred somewhat before the arrival of the main dust cloud on April 25. The leading edge of the dust cloud observed at Salt Lake City was optically too thin to be detected in the satellite imagery, which was seen on April 25 just to the west. The vertical aerosol profile detected by the ruby ($0.694 \mu\text{m}$) polarization lidar [Sassen, 1997] shows a distinct aerosol layer at about 7.5 km altitude (Figure 3). The maximum depolarization of ~ 0.2 in the elevated aerosol layer is unusually high for this location and indicates the presence of supermicron size nonspherical particles of at least $1\text{--}2 \mu\text{m}$ in size [Mishchenko and Sassen, 1998]. The elevated dust layer was noticeable from the ground, produced a solar aureole, and at times resembled very thin cirrus.

The main dust cloud arrived at North America on April 25, 1998. The most noticeable impact of the dust was the discoloration of the sky. Human observer reports and digital photographs indicate that from April 25 onward, the normally blue sky appeared milky white throughout the nonurban West Coast. This effect is due to the redistribution of the direct solar radiation into diffuse skylight. The redistribution effect was well documented through numerous direct/diffuse solar radiation measurements. For example, during the 5 day dust event in Oregon, there was a 25–35% decrease in direct normal solar radiation (Figure 4), although most of the loss from the direct solar beam was still reaching the ground as diffuse skylight. It is quite remarkable, however, that the total broadband radiation reaching a horizontal surface during the dust event was reduced only by about 2%, leaving only 2% for aerosol absorption and backscattering to space. This is consistent with SeaWiFS reflectance data, which indicate that the increase of the surface albedo near Eugene, Oregon, from the dust-free day on April 20 to the dusty day April 27 was below 2%. More extensive analysis [Gueymard *et al.*, 2000] shows that on April 27 the noon direct irradiance at Eugene, Oregon, Burns, Oregon, and Boise, Idaho, was reduced by 28, 31, and 31%, respectively, substantially diminishing the solar energy available for concentrating solar collectors. The noon global hori-

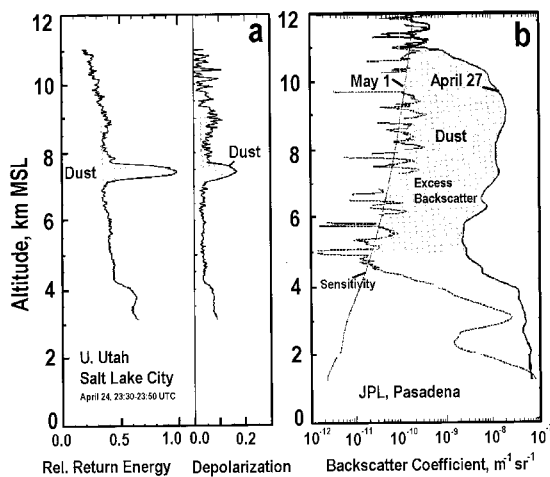


Figure 3. Lidar profiles of the Asian dust cloud over North America. (a) Averaged lidar profiles at Salt Lake City, Utah. The range-normalized returned energy profile (in arbitrary units) shows a strongly scattering aerosol layer between 7 and 8 km. The lidar linear depolarization profile at right has delta values up to 18% in the elevated aerosol layer, indicating nonspherical dust particles. (b) Lidar backscatter profiles at Pasadena, California. The solid curve represents data from April 27, 1998, at the peak of the event. The dashed curve shows the profile at the end of the event on May 1, 1998, when the signal returned to near background conditions. The dust layer is evident between about 5 and 10 km. The dotted curve denotes the system sensitivity.

zonal irradiance was also reduced by 34 W/m^2 (3.8%), 39 W/m^2 (4.1%), and 45 W/m^2 (5.1%), respectively, at these sites, compared to the dust-free conditions.

The arrival of the main dust cloud to North America was evidenced by the Sun photometer data at Reno, Nevada, and San Nicolas Island in southern California. At Reno the aerosol optical thickness ($0.525 \mu\text{m}$) rose sharply on April 25 and remained high ($0.3 < \tau < 0.5$) until April 29, compared to $\tau < 0.1$ on the preceding days [DuBois, 2001]. The optical depth also increased at San Nicolas Island on April 25, reaching a

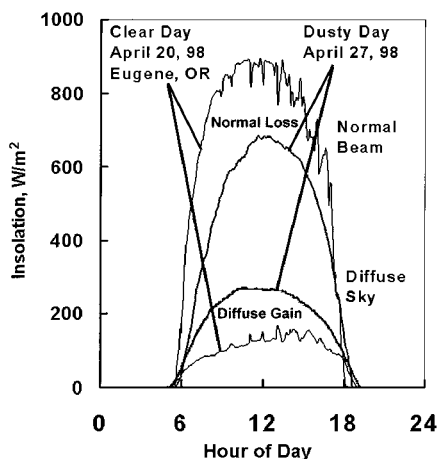


Figure 4. Direct normal and diffuse solar radiation data for Eugene, Oregon, for a dust-free day (April 20, 1998) and a day with dust (April 27, 1998) [Gueymard et al., 2000]. Note the loss of direct radiation and doubling of the midday diffuse radiation due to scattering by dust particles.

peak value of $\tau = 0.5$ at $0.500 \mu\text{m}$ [Tratt et al., this issue]. During the same period over the Pacific Northwest the aerosol optical depth was in the range $0.4 < \tau < 0.5$ (N. S. Laulainen et al., manuscript in preparation, 2000) (hereinafter referred to as L2000).

During the dust event, the slope of the spectral optical depth, i.e., the Angstrom exponent, at the San Nicolas Island and the Pacific Northwest, was below 0.5, which is indicative of supermicron characteristic particle size. On the basis of the inversion of additional Sun and sky radiance measurements at San Nicolas Island, Tratt et al. [this issue] reported a coarse mode diameter of $2\text{--}4 \mu\text{m}$ for the dust. The entire retrieved dust volume distribution is shown in Plate 2e along with the data from Korea. Aircraft measurements through the dust layer near Richland, Washington, on May 1, exhibited a similar volume distribution (L2000). Size-segregated dust samples at numerous remote locations over the Northwest and adjacent Canada showed that about 30–50% of the dust mass was below $2.5 \mu\text{m}$ [McKendry et al., this issue]. These size estimates all indicate that the aged Asian dust arriving at the West Coast had a mass median diameter of about $2\text{--}3 \mu\text{m}$.

A variety of observations over North America indicated the Asian dust has a layered structure. Lidar backscatter data from the Jet Propulsion Laboratory in Pasadena, California (Figure 3b), show the vertical aerosol profiles during the dust event on April 27 and after the event on May 1 [Tratt et al., this issue]. On April 27 a suspected dust layer was apparent between 5 and 10 km altitude where the lidar backscattering was more than 2 orders of magnitude above the nominal background values. Lidar data from Salt Lake City on April 25 show a thin 1 km deep dust layer at 7.5 km height (Figure 3a).

Serendipitous aircraft aerosol sampling on April 27 near Seattle, Washington, showed a distinct dust layer at about 2–3 km altitude (S. Gassó, personal communication, 1999) and virtually no dust below, whereas a subsequent aircraft sounding over eastern Washington State on May 1 indicated a surface-based dust layer up to about 2 km (L2000). Aerosol optical depth (AOD) measurements at two elevations (1088 and 100 m) are consistent with an aerosol scale height of about 2 km.

In southern British Columbia the PM_{10} levels increased dramatically to $\sim 100 \mu\text{g/m}^3$ in the southern interior of the province on April 28. To the west, concentrations peaked in the Lower Fraser Valley (Vancouver region) on April 29 and then farther west on Vancouver Island on April 30. This pattern is consistent with mesoscale modeling of the event [McKendry et al., this issue], showing strong subsidence and downward mixing of the dust layers over the mountainous interior and then westward surface transport of dust in “out-flow” winds. Monitoring of aerosol light scattering at the Cheeka Peak Observatory in Washington State also showed the arrival of the dust cloud on April 28 with an easterly flow (D. A. Jaffe, personal communication, 1999). On the basis of an analysis of elemental composition and meteorological analogs it was estimated that Asian dust contributed 40–50% to peak observed PM_{10} levels in the Vancouver area [McKendry et al., this issue].

The visible channel of the GOES 10 geostationary satellite provided a view of the dust spatial distribution on the evening of April 27 at about 1800 PST (Figure 5a). Evidently, the subsided dust cloud covered the entire west coast of North America from California to British Columbia and a wedge-

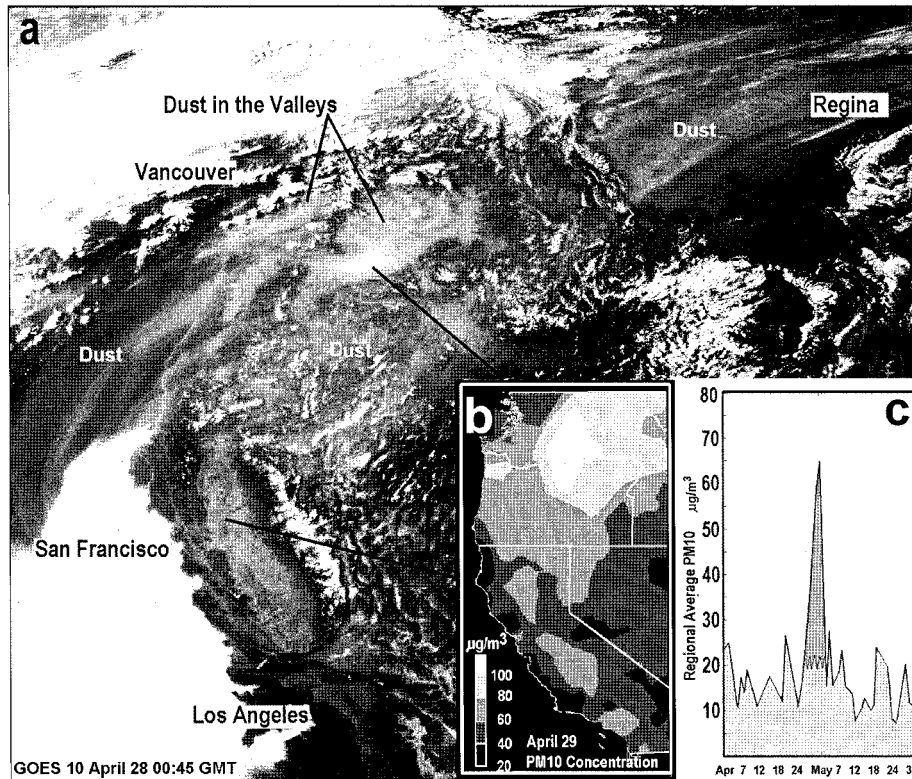


Figure 5. GOES 10 geostationary satellite image of the dust taken on the evening of April 27. The dust cloud, marked by the brighter reflectance, covers the entire northwestern United States and adjacent portions of Canada. A dust stream is also seen crossing the Rocky Mountains toward the east. (b) Contour map of the PM10 concentration on April 29, 1998, based on 230 data points interpolated using the inverse distance squared method. (c) Daily time series of PM10 averaged over the West Coast based on 25 AIRS stations. Note the coincidence of high PM10 and satellite reflectance over eastern Washington State and the sharp rise of the regional average PM10 on April 27.

shaped region of the northwestern United States and adjacent Canada extending well into the center of the continent.

Extensive PM10 monitoring data [U.S. Environmental Protection Agency (EPA), 1994] over the U.S. West Coast provided a relatively detailed spatial map of the surface dust concentrations (Figure 5b) as well as the temporal pattern (Figure 5c). Daily PM10 concentrations averaged over 25 AIRS stations throughout the West Coast show a strong peak between April 26 and May 1 (Figure 5c). During the dust incursion, the average PM10 concentration reached $65 \mu\text{g}/\text{m}^3$ compared to $10\text{--}25 \mu\text{g}/\text{m}^3$ during the remainder of the April-May 1998 period. This suggests that the excess dust concentration over the West Coast reached about $40 \mu\text{g}/\text{m}^3$.

On April 29, the contour map (based on 230 stations) shows that the PM10 concentration over the low-lying areas of California, Nevada, and Idaho also experienced concentrations well above $50 \mu\text{g}/\text{m}^3$. The PM10 concentrations over parts of Washington and Oregon exceeded $100 \mu\text{g}/\text{m}^3$ (Figure 5b). This patch of high dust concentration coincided with the bright aerosol reflectance in the GOES satellite image for April 27. The rough spatial coincidence of satellite and surface data is consistent with the observation that by April 29 the dust layer had subsided to the surface.

The chemical composition of the sampled dust over North America shows that the dust is composed of crustal elements with constant elemental ratios throughout the episode [McKendry *et al.*, this issue]. Aerosol samples collected by aircraft

over Washington State on May 1 were nonvolatile and refractory in nature (L2000), which is consistent with crustal particle composition.

The chemical composition of the Asian dust was also established through the IMPROVE monitoring network data (Figure 6). On the basis of specific dust elemental signatures [Malm *et al.*, 1994] the speciated aerosol data revealed the

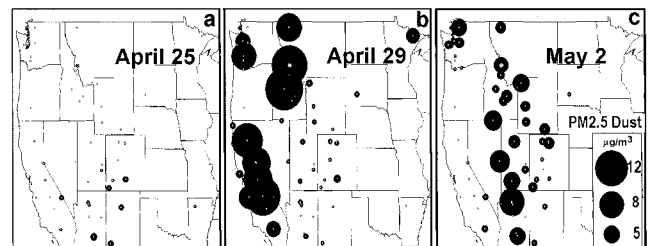


Figure 6. Fine particle dust concentration pattern based on the IMPROVE speciated aerosol data. The dust mass concentration was calculated from the crustal elements based on the formula of Malm *et al.* [1994]. $\text{PM}_{2.5} \text{ dust} = 2.2[\text{Al}] + 2.49[\text{Si}] + 1.63[\text{Ca}] + 2.42[\text{Fe}] + 1.94[\text{Ti}]$. Evidently, on April 25 the dust layer seen by the Sun photometers was still elevated since the surface dust concentration was low. By April 29 the dust subsided to the surface over the West Coast and by May 2 it migrated inland. The total (fine and coarse) dust concentrations were probably 2–3 times above the PM2.5 values.

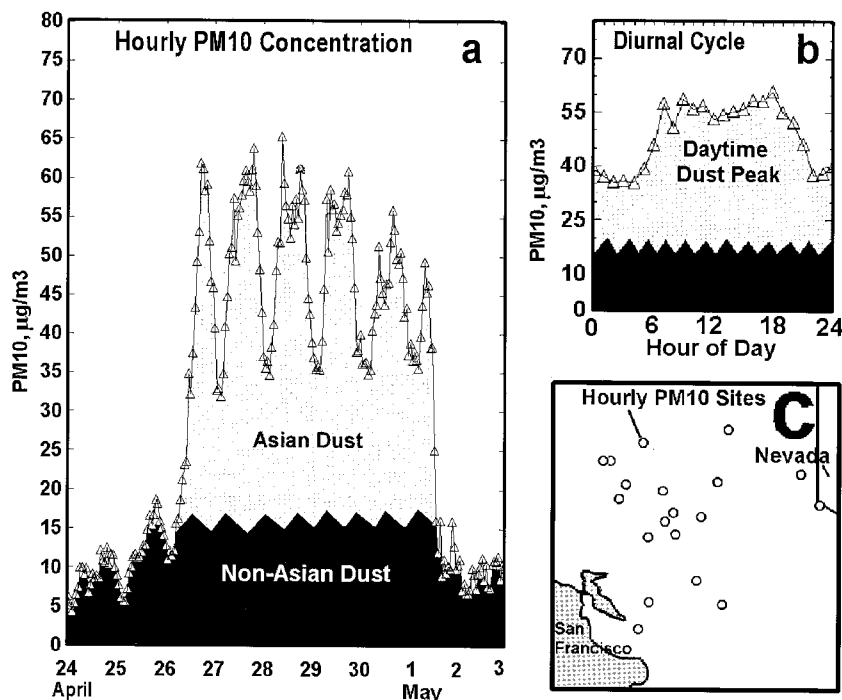


Figure 7. Hourly concentration pattern of PM₁₀. (a) Hourly PM₁₀ concentration averaged over 12 stations in northern California. (b) Diurnal pattern of PM₁₀ averaged over all stations on April 29, 1998. (c) Location of the hourly PM monitoring sites in the San Francisco-Sacramento area. Note the rise of concentration and the strong diurnal cycle during the April 26 to May 1 dust event.

pattern of dust without interference from other local aerosol contributions, such as sulfates, organics, soot, and nitrates. On April 25 the western United States was virtually dust-free (Figure 6a). This means that the rise in the optical depth detected by the Sun photometers at Reno and San Nicolas Island on April 25 was exclusively due to elevated dust layers well separated from the surface.

The dust concentration on the surface reached high levels on April 29, particularly in the Northwest (Figure 6b). By May 2 the dust levels along the coast declined and the elevated dust concentrations were highest over the Rocky Mountains and the Colorado Plateau (Figure 6c). By May 6 the dust levels had declined throughout most of the western United States. Photographs and observations from southeastern Utah taken on May 3–4 also recorded the progress of “strange haze” across the Colorado Plateau, moving from northern Arizona into western Colorado [Reheiss, 1998]. However, this dust transport to the interior of North America has not been confirmed by detailed meteorological analysis.

The IMPROVE network data over North America show that the Asian dust chemical components are not correlated with particulate sulfur during the dust event. In fact, the samples with the highest dust concentrations had virtually no sulfur content. Aircraft sampling of the dust near Richland, Washington, on May 1 showed that the aerosol had no volatile components up to 300°C, which is consistent with a purely soil-derived chemical composition of the dust (L2000). Thus on the basis of the above crude observations there is no evidence that the April 19 dust cloud had significant chemical transformations due to interaction with pollutant species, such as sulfur.

5.5. Dissipation

A unique aspect of the April 19 dust cloud is that there was no evidence of significant wet removal neither during its residence over the Asian continent nor during the trans-Pacific transport. This is inferred from the lack of major precipitating cloud systems over east Asia and the Pacific during the passage.

The partial dissipation of the dust cloud over the West Coast of North America was facilitated by the subsidence of the dust layer from the midtroposphere to the surface, between April 27 and 29 [McKendry *et al.*, this issue]. In British Columbia a zonally oriented jet core to the north of Vancouver helped generate substantial mountain waves and subsidence (~ 0.05 m/s) in the lee of the coast mountain range and the Rocky Mountains. Rapid downward transport permitted interception of dust layers by surface-based mixing and removal processes and then coastward transport by easterly surface winds. As a result of such processes, high surface level dust concentrations, lasting from April 27 until May 1, were observed over much of the northwestern United States and adjacent Canada.

Hourly PM₁₀ concentration data averaged over 12 stations in northern California show a strong and consistent diurnal cycle throughout the Asian dust episode between April 26 and May 2 (Figure 7a). Following the sharp concentration rise on April 26, there was a daily modulation with a peak of about $55 \mu\text{g}/\text{m}^3$ during the daytime hours (0700–1900) and a decline to $35 \mu\text{g}/\text{m}^3$ at night. The diurnal modulation is evidence for the presence of a stable dust reservoir that remained aloft in the boundary layer for 6 days and was well mixed to the surface during the daytime. Possibly, the surface concentrations de-

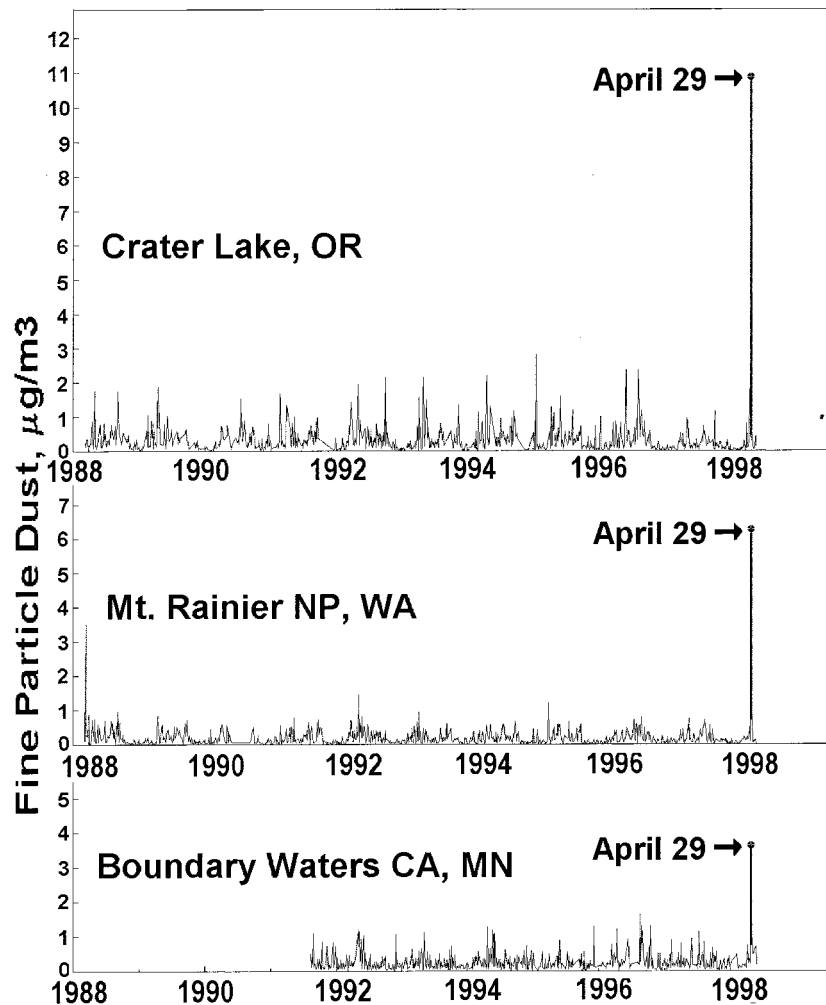


Figure 8. Ten-year trend of PM_{2.5} dust concentration at three IMPROVE monitoring sites. The fine-particle dust mass was reconstructed from the concentration of crustal elements. The simultaneous sharp rise at all three sites on April 29 marks the dust event. Evidently, the April 1998 Asian dust event caused 2–4 times higher dust concentrations than any other event during 1988–1998.

clined at night, since particles were removed by dry deposition within the shallow nocturnal layer slowly depleting the dust reservoir aloft. [Wilson and Stockburger, 1990].

The ultimate fate of the entire dust cloud reaching North America is not known, but there is evidence that part of the dust was transported eastward across the continent. Near the U.S.-Canadian border, streaks of dust indicate swift transport toward the upper Midwest and Ontario (Figure 5a). A second stream turned toward the south, blanketing the West Coast from British Columbia to California. The stream of Asian dust was visually and chemically detectable to Minnesota, and it is probable that its eastward transport was unhindered until the dust reached the 3000 m plateau of Greenland, where much of the high-latitude precipitation takes place. These observations of dust transport support the Asian origin of the dust deposited in the Greenland ice sheet over geological times [Biscaye *et al.*, 1997].

6. Discussion

The remarkable high dust concentrations over North America reported here raise the question of frequency at which such

trans-Pacific dust transport events take place. Evidently, the April 1998 Asian dust transport to North America was a rare event. Figure 8 shows the daily PM_{2.5} dust concentration at three IMPROVE monitoring sites for which long-term records exist: Mount Rainier, Washington, Crater Lake, Oregon, and Boundary Water, Minnesota. On the basis of the characteristic dust size of 2–3 μm it can be estimated that the total dust mass concentration was 2–3 times higher than the PM_{2.5} dust concentration.

At each site, the fine particle dust concentration was variable but generally below 5 $\mu\text{g}/\text{m}^3$ throughout the decade of 1988–1998. The exception is the sharp dust peak at each of these sites reaching 5–10 $\mu\text{g}/\text{m}^3$ on April 29, 1998. Hence the April 1998 Asian dust event was 2–4 times more intense than any other dust incursion to the western United States over the past decade.

The Asian dust storms of April 1998 had major consequences to human health and welfare. According to CNN, on April 15, 12 people perished in the dust storm in the Xinjiang Autonomous Region of China alone. It is probable that this natural disaster has caused additional casualties along its path.

Yellow muddy rain, reported over eastern China and Korea, produced an economic loss of unknown magnitude.

When the dust cloud reached British Columbia, Washington, Idaho, and Oregon, the respective state health agencies issued air pollution advisory warnings to the general public with a corresponding ban on open prescribed burning. In making their decisions and informing the public the state air pollution regulatory agencies actively participated in the virtual community by supplying and using information on the Asian Dust web site.

Such dust events have both research and regulatory implications. With a measured mass mean diameter of 2–3 μm the dust will influence the fine PM_{2.5} concentration as well as PM₁₀ concentrations. This is important since there is increasing information to suggest that at least for some health effects categories, fine-mode particles are more likely to cause acute health effects than coarse-mode soil particles [Schwartz *et al.*, 1997, 1999]. Therefore episodic intrusions of soil dust need to be identified not only to allow waivers for possible exceedances of the PM_{2.5} and PM₁₀ standards but also to correct PM_{2.5} time series for use in correlation of fine-mode particles with health effects.

The available routine and the limited serendipitous dust observations used in this paper (e.g., mass loading, particle size and chemical composition, aerosol optical thickness, dust layer height) have been useful for elucidating some features of the two Asian dust events in April 1998. However, a firm and full quantitative characterization of these events, particularly the physicochemical processes, was not possible since many of the necessary measurements were not made. In addition, it is not clear how representative the April 1998 events were. The planned ACE-Asia studies (<http://saga.pmel.noaa.gov/aceasia>) beginning in 2001 are expected to characterize the east Asian aerosol properties over time and above the surface and quantify the transport, transformations, and fate of these aerosols.

The Asian dust event has demonstrated that the currently available space-borne and surface aerosol monitoring can enable virtual communities of scientists and regulatory bodies to detect and follow such major aerosol events, whether resulting from fires, volcanoes, pollution, or dust storms. It has also been shown that ad hoc collaboration of scientists is a practical way to share observations and to collectively generate the explanatory knowledge about such unpredictable events. The experience from this event could also help in more effectively planning disaster mitigation efforts, such as an early detection, warning, and analysis system.

Additional work on the April 1998 dust events could include (1) organizing the available data into a documented and shared resource base, (2) a coordinated global dynamic aerosol model validation, and testing programs, (3) explaining the yellow dust color, and (4) additional collaborative data integration and fusion and analysis. In the future a web-based communication, cooperation, and coordination system would be useful to monitor the global aerosol pattern for unusual or extreme aerosol events. The system would alert and inform the interested communities so that the detection and analysis of such events is not left to serendipity. It is envisioned that such a community-supported global aerosol information network be open to a broad international participation, complement and synergize with other monitoring programs and field campaigns, and support the scientific as well as the air quality and disaster management communities.

Acknowledgments. The authors thank the virtual community that assembled on the dust website for sharing their observations and ideas. In particular, the assistance of Larry Altose, Air Quality Program, Washington State DNR, Steven Sakiyama, British Columbia Ministry of Environment, Lands and Parks, ARB and State of Idaho DEQ are gratefully acknowledged. During the dust event, Maja Husar maintained the CAPITA Asian Dust website and Janja Husar contributed to the preparation of the manuscript. We also thank one of the reviewers for suggesting a chronological organization of the paper. Portions of this work were carried out at the Jet Propulsion Laboratory, California Institute of Technology, under contract with the National Aeronautics and Space Administration. The CAPITA part of this research was funded in part by the U.S. Environmental Protection Agency (EPA) through CX-825834 (OAR-OAQPS). Mention of trade names or commercial products does not constitute endorsement or recommendation for use.

References

- Bachmeier, S., Asian Dust Over the Pacific Ocean, <http://cimss.ssec.wisc.edu/goes/misc/980424.html>, CIMSS, Univ. of Wisconsin, Madison, Wisc., 1998.
- Barnes, R. A., R. E. Eplee Jr., F. S. Patt, and C. R. McClain, Changes in the radiometric sensitivity of SeaWiFS, *Appl. Opt.*, **38**(21), 4649–4664, 1999.
- Biscaye, P. E., F. E. Grousset, M. Revel, S. VanderGaast, G. A. Zielinski, A. Vaars, and G. Kukla, Asian provenance of glacial dust (stage 2) in the Greenland Ice Sheet Project 2 Ice Core, Summit, Greenland, *J. Geophys. Res.*, **102**, 26,765–26,781, 1997.
- Bodhaine, B. A., Aerosol absorption measurements at Barrow, Mauna Loa, and the South Pole, *J. Geophys. Res.*, **100**, 8967–8975, 1995.
- Chadwick, O. A., L. A. Derry, P. M. Vitousek, B. J. Huebert, and L. O. Hedin, Changing sources of nutrients during four million years of ecosystem development, *Nature*, **397**, 491–497, 1999.
- Christensen, J. H., The Danish eulerian hemispheric model—A three-dimensional air pollution model used for the Arctic, *Atmos. Environ.*, **31**, 4169–4191, 1997.
- Chun, Y. S., Synopsis, transport, and physical characteristics of Asian dust in Korea, *J. Geophys. Res.*, this issue.
- Chun, Y., J. Kim, J. C. Choi, K. O. Boo, M. Lee, and S. N. Oh, Characteristic number size distribution of aerosol during Asian dust episode in Korea, *Atmos. Environ.*, in press, 2000.
- DuBois, D., Application of particulate matter monitoring network design, Ph.D. dissertation, Univ. of Nevada, Reno, 2001.
- Duce, R. A., C. K. Unni, B. J. Ray, J. M. Prospero, and J. T. Merrill, Long-range atmospheric transport of soil dust from Asia to the tropical North Pacific: Temporal variability, *Science*, **209**, 1522–1524, 1980.
- Dymond, J., P. E. Biscaye, and R. W. Rex, Eolian origin of mica in Hawaiian soils, *Geol. Soc. Am. Bull.*, **85**, 37–40, 1974.
- Gillette, D., A wind tunnel simulation of the erosion of soil: Effect of soil texture, sand-blasting, wind speed, and soil consolidation on the dust production, *Atmos. Environ.*, **12**, 1735–1743, 1978.
- Gueymard, C. A., C. N. S. Laulainen, J. K. Vaughan, and F. E. Vignola, China's dust affects solar resource in the U.S.: A case study, SOLAR 2000, paper presented at the ASES Annual Conference, U.S. Dep. of Energy, Madison, Wisc., June 16–21, 2000.
- Herman, J. R., P. K. Bhartia, O. Torres, C. Sefator, and E. Celarier, Global distribution of UV-absorbing aerosols from Nimbus 7/TOMS data, *J. Geophys. Res.*, **102**, 16,911–16,922, 1997.
- Hogan, T. F., and T. E. Rosmond, The description of the Navy operational global atmospheric prediction system's spectral forecast model, *Mon. Weather Rev.*, **119**, 1786–1815, 1991.
- Holben, B. N., et al., AERONET—A federated instrument network and data archive for aerosol characterization, *Remote Sens. Environ.*, **66**, 1–16, 1998.
- Husar, R. B., J. M. Prospero, and L. L. Stowe, Characterization of tropospheric aerosols over the oceans with the NOAA advanced very high resolution radiometer optical thickness operational product, *J. Geophys. Res.*, **102**, 16,889–16,909, 1997.
- Iwasaka, Y., H. Minoura, and K. Nagaya, The transport and spatial scale of Asian dust-storm clouds: A case study of the dust-storm event of April 1979, *Tellus, Ser. B*, **35**, 189–196, 1983.
- Jaffe, D. A., A. Mahura, J. Kelley, J. Atkins, P. C. Novelli, and J. Merrill, Impact of Asian emissions on the remote North Pacific atmosphere: Interpretation of CO data from Shemya, Guam, Midway, and Mauna Loa, *J. Geophys. Res.*, **102**, 28,627–28,636, 1997.

- Jaffe, D. A., et al., Transport of Asian air pollution to North America, *Geophys. Res. Lett.*, 26, 711–714, 1999.
- Kennedy, M. J., O. A. Chadwick, P. M. Vitousek, L. A. Derry, and D. M. Hendricks, Changing sources of base cations during ecosystem development, Hawaiian Islands, *Geology*, 26, 1015–1018, 1998.
- King, M. D., Y. J. Kaufman, D. Tanre, and T. Nakajima, Remote sensing of tropospheric aerosols from space: Past, present and future. *Bull. Am. Meteorol. Soc.*, 80, 12,229–12,259, 1999.
- Korean Meteorological Research Institute (KMRI), The characterization of aerosol related to yellow sand phenomena in Korea, *Tech. Rep. MR990A20*, 143 pp., Seoul, 1999.
- Kuring, N., SeaWiFS observes transport of Asian dust over the Pacific Ocean, http://daac.gsfc.nasa.gov/CAMPAIGN_DOCS/OCDST/asian_dust.html, NASA Goddard Space Flight Cent., Greenbelt, Md., 1998.
- Malm, W. C., J. F. Sisler, D. Huffman, R. A. Eldred, and T. A. Cahill, Spatial and seasonal trends in particle concentration and optical extinction in the United States, *J. Geophys. Res.*, 99, 1347–1370, 1994.
- McClain, C. R., M. L. Cleave, G. C. Feldman, W. W. Gregg, S. B. Hooker, and N. Kuring, Science quality SeaWiFS data for global biospheric research, *Sea Technol.*, 39, 10–16, 1998.
- McKendry, I. G., J. P. Hacker, R. Stull, S. Sakiyama, D. Mignacca, and K. Reid, Long-range transport of Asian dust to the Lower Fraser Valley, British Columbia, Canada, *J. Geophys. Res.*, this issue.
- Merrill, J. T., M. Uematsu, and R. Bleck, Meteorological analysis of long range transport of mineral aerosols over the North Pacific, *J. Geophys. Res.*, 94, 8584–8598, 1989.
- Mishchenko, M. I., and K. Sassen, Depolarization of lidar returns by small ice crystals: An application to contrails, *Geophys. Res. Lett.*, 25, 309–312, 1998.
- Mizohata, A., and T. Mamuro, Some information about loess aerosol over Japan, *Jpn. Soc. Air Pollut.*, 13, 289–297, 1978.
- Murayama, T., et al., Lidar network observation of Asian dust in Japan, *Proc. SPIE*, 3504, 8–15, 1998.
- Murayama, T., et al., Ground-based network observation of Asian dust events of April 1998 in east Asia, *J. Geophys. Res.*, this issue.
- National Climate Data Center (NCDC), Global Surface Summary of Day, <http://www.ncdc.noaa.gov/>, Natl. Clim. Data Cent., Asheville, N.C., 1998.
- Nickovic, S., G. Kallos, A. Papadopoulos, and O. Kakaliagou, Model for prediction of desert dust cycle in the atmosphere, *J. Geophys. Res.*, this issue.
- Parrington, J. R., W. H. Zoller, and N. K. Aras, Asian dust: Seasonal transport to the Hawaiian Islands, *Science*, 220, 195–197, 1983.
- Prospero, J. M., and D. L. Savoie, Effect of continental sources of nitrate concentrations over the Pacific Ocean, *Nature*, 339, 687–689, 1989.
- Reheiss, M., Possible sighting of Asian dust in eastern Utah, <http://climchange.cr.usgs.gov/info/dust/gobi/>, USGS, Geol. Div. Cent. Reg., Denver, Colo., 1998.
- Rex, R. W., J. K. Syers, M. L. Jackson, and R. N. Clayton, Eolian origin of quartz in soils of Hawaiian Islands and in Pacific pelagic sediments, *Science*, 163, 277–291, 1969.
- Sassen, K., Contrail-cirrus and their potential for regional climate change, *Bull. Am. Meteorol. Soc.*, 78, 1885–1903, 1997.
- Schwartz, J., D. W. Dockery, and L. M. Neas, Is daily mortality associated specifically with fine particles?, *J. Air Waste Manage. Assoc.*, 46, 927–939, 1997.
- Schwartz, J., G. Norris, T. Larson, L. Sheppard, C. Claiborne, and J. Koenig, Episodes of high coarse particle concentrations are not associated with increased mortality, *Environ. Health Perspect.*, 107, 339–342, 1999.
- Shaw, G. E., Transport of Asian desert aerosol to the Hawaiian Islands, *J. Appl. Meteorol.*, 19, 1254–1259, 1980.
- Symons, G. J. (Ed.), *The Eruption of Krakatoa and Subsequent Phenomena*, Harrison and Sons, Truebner & Co., London, 1888.
- Talbot, R. W., et al., Chemical characteristics of continental outflow from Asia to the troposphere over the western Pacific Ocean during February–March 1994: Results from PEM West-B, *J. Geophys. Res.*, 102, 28,255–28,274, 1997.
- Tratt, D. M., and R. T. Menzies, Recent climatological trends in atmospheric aerosol backscatter derived from the Jet Propulsion Laboratory multiyear backscatter profile database, *Appl. Opt.*, 33(3), 424–430, 1994.
- Tratt, D. M., R. J. Frouin, and D. L. Westphal, April 1998 Asian dust event: A southern California perspective, *J. Geophys. Res.*, this issue.
- Uematsu, M., R. A. Duce, J. M. Prospero, L. Chen, J. T. Merrill, and R. L. McDonald, Transport of mineral aerosol from Asia over the North Pacific Ocean, *J. Geophys. Res.*, 88, 5343–5352, 1983.
- U.S. Environmental Protection Agency (EPA), *AIRS User's Guide*, vol. AQ1, AQS data dictionary, *EPA-454/B-94-005*, Washington, D. C., 1994.
- Vermote, E., and D. Tanre, Analytical expression for radiative properties of planar Rayleigh scattering media, including polarization, *J. Quant. Spectrosc. Radiat. Transfer*, 47(4), 305–314, 1992.
- Wang, M. X., J. W. Winchester, T. A. Cahill, and L. X. Ren, Chemical elemental composition of windblown dust, 19 April 1980, Beijing, *Kexue Tongbao*, 27, 1193–1198, 1982.
- Westphal, D. L., Real-time applications of a global multicomponent aerosol model, *J. Geophys. Res.*, in press, 2000.
- Wilson, W. E., and L. Stockburger, Diurnal variations in aerosol composition and concentration in aerosols: Science, industry, health, and environment, in *Proceedings of the Third International Aerosol Conference*, edited by S. Masuda and K. Takahashi, pp. 962–965, Pergamon, New York, 1990.
- Zaizen, Y., M. Ikegami, K. Okada, and Y. Makino, Aerosol concentration observed at Zhangye in China, *J. Meteorol. Soc. Jpn.*, 73, 891–897, 1995.
- Zhang, D., and F. Lu, Winter sandstorm events in extensive northern China (in Chinese), *Quat. Sci.*, 5, 441–447, 1999.
- Zheng, X., F. Lu, X. Fang, Y. Wang, and L. Guo, A study of dust storms in China using satellite data, in *Optical Remote Sensing of the Atmosphere and Clouds*, edited by J. Wang, B. Wu, T. Ogawa, and Z. Guan, *Proc. SPIE*, 3, 501, 163–168, 1998.
- Zhou, M., Q. Shaohou, S. Ximing, and L. Yuying, Properties of the aerosols during a dust storm over Beijing area, *Acta Sci. Circumstantiae*, 1, 207–219, 1981.
- S. R. Falke, R. B. Husar, F. Li, and B. A. Schichtel, Center for Air Pollution Impact and Trend Analysis, Campus Box 1124, Washington University, St. Louis, MO 63130. (rhusar@me.wustl.edu)
- D. M. Tratt, Jet Propulsion Laboratory, California Institute of Technology, Pasadena, CA 91109.
- S. Gasso and D. Jaffe, Atmospheric Sciences, University of Washington, Seattle, WA 98195.
- T. Gill, Department of Geosciences, Texas Tech University, Lubbock, TX 79409.
- N. S. Laulainen, Pacific Northwest National Laboratory, Richland, WA 99352.
- F. Lu, National Satellite Meteorological Center, China Meteorological Administration, Beijing, China.
- M. C. Reheis, U.S. Geological Survey, Denver, CO 80225.
- Y. Chun, Meteorological Research Institute, Seoul, Republic of Korea.
- D. Westphal, Naval Research Laboratory, Monterey, CA 93943.
- G. C. Feldman, B. N. Holben, N. Kuring, and C. McClain, NASA Goddard Space Flight Center, Greenbelt, MD 20771.
- C. Gueymard, University of Central Florida, Orlando, FL 32816.
- I. McKendry, Department of Geography, University of British Columbia, Vancouver, Canada.
- R. J. Frouin, Scripps Institution of Oceanography, University of San Diego, La Jolla, CA 92110.
- J. Merrill, Center for Atmospheric Chemistry Studies, University of Rhode Island, Kingston, RI 02881.
- D. DuBois, Air Quality Bureau, New Mexico Environment Department, Santa Fe, NM 87505.
- F. Vignola, Solar Monitoring Laboratory, University of Oregon, Eugene, OR 97403.
- T. Murayama, Department of Physics, Tokyo University of Mercantile Marine, Tokyo, Japan.
- S. Nickovic, Euro-Mediterranean Centre on Insular Coastal Dynamics (ICoD), University of Malta, Valletta, Malta.
- W. E. Wilson, National Center for Environmental Assessment, U.S. EPA, Research Triangle Park, NC 27711.
- K. Sassen, Department of Meteorology, University of Utah, Salt Lake City, UT 84112.
- N. Sugimoto, National Institute for Environmental Studies, Tsububa, Ibaraki, Japan.
- W. C. Malm, NPS Air Resources Division, CIRA, Colorado State University, Fort Collins, CO 80521.

(Received July 19, 2000; revised November 14, 2000; accepted November 14, 2000.)